

## Probing the Salmeterol Binding Site on the $\beta_2$ -Adrenergic Receptor Using a Novel Photoaffinity Ligand, [ $^{125}$ I]Iodoazidosalmeterol<sup>†</sup>

Yajing Rong,<sup>‡</sup> Marty Arbabian,<sup>‡</sup> David S. Thiriot,<sup>‡</sup> Anita Seibold,<sup>§</sup> Richard B. Clark,<sup>§</sup> and Arnold E. Ruoho<sup>\*,‡</sup>

Department of Pharmacology, University of Wisconsin—Madison Medical School, 1300 University Avenue, Madison, Wisconsin 53706-1532, and Graduate School of Biomedical Sciences and Department of Pharmacology, University of Texas Health Science Center at Houston, Houston, Texas 77225-0334

Received May 11, 1999; Revised Manuscript Received July 2, 1999

**ABSTRACT:** Salmeterol is a long-acting  $\beta_2$ -adrenergic receptor ( $\beta_2$ AR) agonist used clinically to treat asthma. In addition to binding at the active agonist site, it has been proposed that salmeterol also binds with very high affinity at a second site, termed the “exosite”, and that this exosite contributes to the long duration of action of salmeterol. To determine the position of the phenyl ring of the aralkyloxyalkyl side chain of salmeterol in the  $\beta_2$ AR binding site, we designed and synthesized the agonist photoaffinity label [ $^{125}$ I]-iodoazidosalmeterol ([ $^{125}$ I]IAS). In direct adenylyl cyclase activation, in effects on adenylyl cyclase after pretreatment of intact cells, and in guinea pig tracheal relaxation assays, IAS and the parent drug salmeterol behave essentially the same. Significantly, the photoreactive azide of IAS is positioned on the phenyl ring at the end of the molecule which is thought to be involved in exosite binding. Carrier-free radioiodinated [ $^{125}$ I]IAS was used to photolabel epitope-tagged human  $\beta_2$ AR in membranes prepared from stably transfected HEK 293 cells. Labeling with [ $^{125}$ I]IAS was blocked by 10  $\mu$ M (–)-alprenolol and inhibited by addition of GTP $\gamma$ S, and [ $^{125}$ I]IAS migrated at the same position on an SDS–PAGE gel as the  $\beta_2$ AR labeled by the antagonist photoaffinity label [ $^{125}$ I]iodoazidobenzylpindolol ([ $^{125}$ I]IABP). The labeled receptor was purified on a nickel affinity column and cleaved with factor Xa protease at a specific sequence in the large loop between transmembrane segments 5 and 6, yielding two peptides. While the control antagonist photoaffinity label [ $^{125}$ I]IABP labeled both the large N-terminal fragment [containing transmembranes (TMs) 1–5] and the smaller C-terminal fragment (containing TMs 6 and 7), essentially all of the [ $^{125}$ I]IAS labeling was on the smaller C-terminal peptide containing TMs 6 and 7. This direct biochemical evidence demonstrates that when salmeterol binds to the receptor, its hydrophobic aryloxyalkyl tail is positioned near TM 6 and/or TM 7. A model of IAS binding to the  $\beta_2$ AR is proposed.

The transmembrane (TM)<sup>1</sup> domains of the  $\beta_2$ -adrenergic receptor ( $\beta_2$ AR) contain binding determinants for the interaction of antagonists and agonists. A coordinated interaction of the catechol and amino groups of catecholamines with side chains of amino acids in TM 5 (postulated to be Ser 204 and Ser 207) and TM 3 (Asp 113) has been suggested as the primary binding determinants for several *N*-aralkyl derivatives of agonists and antagonists which bind with high affinity to the  $\beta_2$ AR. One component of this interaction of ligands in the  $\beta_2$ AR binding site may involve molecules in folded conformations, as suggested for the antagonist photolabel [ $^{125}$ I]iodoazidobenzylpindolol ([ $^{125}$ I]IABP) (1).

Salmeterol, an analogue of albuterol, is a long-acting  $\beta_2$ -AR agonist substituted with an *N*-aralkyl ether that appears

to exhibit unusually slow dissociation kinetics for dissociation from the  $\beta_2$ AR (2). The coupling efficiency of salmeterol has indicated that it is a partial agonist with regard to  $\beta_2$ -AR-mediated adenylyl cyclase activation in HEK 293 cell membranes which contain overexpressed human  $\beta_2$ AR (3), as well as in other systems. These studies demonstrated that the extent of salmeterol-induced desensitization was greatly reduced compared to that of epinephrine, which was consistent with partial agonist properties and prolonged activation of adenylyl cyclase (3, 4). It was also shown that salmeterol binding to the active site was readily reversible and competitive with  $\beta_2$ AR ligands and displayed a  $K_d$  of 1–2 nM (3, 5).

In addition to regular catechol binding interactions, it has been proposed that salmeterol interacts at an additional site, which has been termed the “exosite” (2). This model proposes that salmeterol is tethered via its aryloxyalkyl side chain to the exosite with extremely high affinity, and that this site serves as an anchor to maintain salmeterol in the binding site or close to the receptor, even after addition of antagonist reverses the functional effects of salmeterol. Evidence in support of this was recently reported by Green et al. (5) and involved studies of  $\beta_1$ - and  $\beta_2$ AR chimeras. Binding and washout studies using  $\beta_1/\beta_2$  chimeric receptors

<sup>†</sup> This work was supported by NIH Grants GM33138 (A.E.R.) and GM21308 (R.B.C.), with additional funding from Glaxo Wellcome Inc. D.S.T. received support from the University of Wisconsin—Madison NIH-sponsored Chemistry-Biology Interface Training Grant.

<sup>\*</sup> To whom correspondence should be addressed. E-mail: aeruoho@facstaff.wisc.edu. Phone: (608) 263-5382. Fax: (608) 262-1257.

<sup>‡</sup> University of Wisconsin—Madison Medical School.

<sup>§</sup> University of Texas Health Science Center at Houston.

<sup>1</sup> Abbreviations: TM, transmembrane;  $\beta_2$ AR,  $\beta_2$ -adrenergic receptor; IABP, iodoazidobenzylpindolol; IAS, iodoazidosalmeterol; PT, proximal trachea; DT, distal trachea; AMS, aminosalmerol; AZS, azidosalmeterol; AIS, azidoiodosalmeterol.

suggested that a 10-amino acid sequence in putative TM 4 (amino acids 149–158) is involved in some fashion in exosite binding of salmeterol on the  $\beta_2$ AR. An alternative hypothesis (6) suggested that the quasi-irreversible properties of the exosite could be due to the highly lipophilic character of salmeterol (7, 8), and recent kinetic studies (9) may support this proposal. The study of the molecular recognition involved in exosite binding is of significant interest and may lead to the design of additional G-protein-coupled receptor ligands with long-acting properties.

In our studies, we have taken a direct biochemical approach using photoaffinity labeling to investigate the salmeterol binding site on human  $\beta_2$ AR. A unique synthetic scheme for the synthesis of several derivatives of salmeterol has been demonstrated on the basis of a newly devised synthetic strategy (10). A novel agonist photoaffinity label, [<sup>125</sup>I]iodoazidosalmeterol ([<sup>125</sup>I]IAS), was developed in which the photoactive azide group is positioned on the phenyl ring at the end of the aralkyloxyalkyl chain, which is the part of the salmeterol molecule that confers exosite binding properties. IAS was tested to show that it retained the pharmacological properties of the parent drug, salmeterol. For human  $\beta_2$ AR expressed in HEK 293 cells, IAS showed similar direct adenylyl cyclase activation and caused a similar effect on adenylyl cyclase activity following drug pretreatment, as salmeterol itself. The dose–response curves obtained for relaxation of carbachol-contracted guinea pig trachea and drug washout times are also similar for salmeterol and IAS.

Carrier-free [<sup>125</sup>I]IAS has been synthesized and shown to specifically label the  $\beta_2$ AR. Labeling with [<sup>125</sup>I]IAS was blocked by 10  $\mu$ M (–)-alprenolol and inhibited by addition of GTP $\gamma$ S and migrated at the same position on an SDS–PAGE gel as  $\beta_2$ AR labeled with the antagonist photoaffinity label [<sup>125</sup>I]IABP. Labeled receptor was purified by nickel affinity chromatography and cleaved with factor Xa protease at a specific sequence in the large loop between transmembrane segments 5 and 6, yielding two peptides. While the control antagonist photoaffinity label [<sup>125</sup>I]IABP labeled both the large N-terminal fragment (containing TMs 1–5) and the smaller C-terminal fragment (containing TMs 6 and 7), essentially all of the [<sup>125</sup>I]IAS labeling was on the smaller C-terminal peptide. This direct biochemical evidence suggests that the salmeterol aryloxyalkyl side chain is on the  $\beta_2$ AR positioned near the region containing TM 6 and/or TM 7.

## MATERIALS AND METHODS

All solvents were reagent grade, except where indicated. Na<sup>125</sup>I (2200 Ci/mmol) was purchased from Du Pont-NEN. Other chemical reagents were obtained from Sigma or Aldrich. Factor Xa protease was purchased from Promega (Madison, WI). Centricon concentrators were from Amicon (Beverly, MA). IR spectra were recorded on a Perkin-Elmer 180 spectrometer. Proton nuclear magnetic resonance spectra were recorded on a Bruker 300 MHz spectrometer. Mass spectra were obtained on a Kratos MS-80RFA with a DS55/DS90 spectrometer. Preparative thin-layer and analytical thin-layer chromatography were performed on precoated Merck Silica Gel 60F-254 glass-backed plates.

*Synthesis of 5-(Bromoacetyl)-2-hydroxybenzaldehyde and 4-[(6-Bromohexyl)oxy]butylbenzene 1.* This synthesis was

carried out by exactly following the procedure described previously (10).

*Synthesis of 4-[4-[(6-Bromohexyl)oxy]butyl]nitrobenzene 2.* To a solution of **1** (315 mg, 1 mmol) in dry MeCN (15 mL) at 0 °C under nitrogen was added dropwise nitronium tetrafluoroborate (160 mg, 1.2 mmol) in dry MeCN (5 mL). The reaction mixture was stirred at 0 °C for 2 h and then poured into a mixture of ice and water. The aqueous layer was extracted with Et<sub>2</sub>O (3  $\times$  50 mL); the organic fractions were combined, washed with brine (50 mL), dried (MgSO<sub>4</sub>), and concentrated on a rotary evaporator. The residue was purified by silica gel column chromatography and eluted with hexanes/ethyl acetate (10:2) to give *p*-nitro compounds (158 mg, 44%) as an oil: IR 1530, 1350 cm<sup>–1</sup> (NO<sub>2</sub>); <sup>1</sup>H NMR (CDCl<sub>3</sub>)  $\delta$  1.30–1.75 (m, 12H), 2.75 (t, *J* = 7.0 Hz, 2H), 3.45 (m, 6H), 7.35 (d, *J* = 10.0 Hz, 2H), 8.15 (d, *J* = 10.0 Hz, 2H); MS (*m/z*) 360 (M<sup>+</sup> + 2), 358 (M<sup>+</sup>).

*Synthesis of N-[6-[4-(4-Nitrophenyl)butoxy]hexyl]benzene-methanamine 3.* To a stirred solution of the above ether **2** (360 mg, 1.0 mmol) in DMSO (5 mL) were added benzylamine (214 mg, 2.0 mmol), triethylamine (101 mg, 1.0 mmol), and NaI (9.0 mg). The mixture was stirred for 15–16 h at room temperature, and then ether (50 mL), 10% NaOH (10 mL), and brine (10 mL) were added. The organic phase was washed with brine. The recovered product was purified by silica gel chromatography (eluted with 10:1 CH<sub>2</sub>Cl<sub>2</sub>/MeOH) to give the required amine **3** as a yellow oil (338 mg, 62%): <sup>1</sup>H NMR (CDCl<sub>3</sub>)  $\delta$  1.25–1.70 (m, 12H), 2.65 (t, *J* = 7 Hz, 2H), 2.75 (t, *J* = 7 Hz, 2H), 3.45 (m, 4H), 3.80 (s, 2H), 7.35–7.40 (m, 7H), 8.15 (d, *J* = 10 Hz, 2H); MS (*m/z*) 384 (M<sup>+</sup>).

*Synthesis of 2-Hydroxy-5-[[[6-[4-(4-nitrophenyl)butoxy]hexyl]benzyl]amino]acetyl]benzaldehyde 4.* A solution of **3** (154 mg, 0.4 mmol) and 5-(bromoacetyl)-2-hydroxybenzaldehyde (48.6 mg, 0.2 mmol) in MeCN (20 mL) or 2-propanol (20 mL) was refluxed for 1 h. After addition of 20 mL of Et<sub>2</sub>O, the mixture was chilled and the precipitated solid was filtered. The filtrate was evaporated, and the residue was chromatographed on a silica gel column (eluted with CH<sub>2</sub>Cl<sub>2</sub>/MeOH) to give **4** (78 mg, 71%) as a yellow oil: IR (film) 1650 cm<sup>–1</sup>; <sup>1</sup>H NMR (CD<sub>3</sub>OD)  $\delta$  1.25–1.75 (m, 12H), 2.53–2.70 (m, 4H), 3.40–3.45 (m, 4H), 3.75 (s, 4H), 6.85 (s, 1H), 7.10–7.25 (m, 5H), 7.35 (d, *J* = 10 Hz, 2H), 7.95–8.10 (m, 2H), 8.15 (d, *J* = 10 Hz, 2H), 9.75 (s, 1H); MS (FAB) 569 (M<sup>+</sup> + H + Na), 547 (M<sup>+</sup> + H).

*Synthesis of Aminosalmeterol 5 (AMS).* NaBH<sub>4</sub> (11 mg, 0.3 mmol) was added slowly to a solution of **4** (55 mg, 0.1 mmol) in MeOH (10 mL) at 0 °C. After being stirred for 36 h at room temperature, the mixture was acidified with 3 N HCl (2 mL) and the solvent removed under reduced pressure. The aqueous phase was adjusted to pH 8 with a 10% Na<sub>2</sub>CO<sub>3</sub> solution and extracted with EtOAc. The extract was washed with H<sub>2</sub>O, dried, and concentrated. The residual oil was diluted with MeOH (10 mL) and hydrogenated in the presence of 10% Pd-C (5 mg) for 10 h. Removal of the catalyst and solvent left an amber syrup which was purified by silica gel chromatography (CH<sub>3</sub>OH/CH<sub>2</sub>Cl<sub>2</sub>) to give an oil **5** (26 mg, 60%): IR 3300–3000 cm<sup>–1</sup> (br); <sup>1</sup>H NMR (CDCl<sub>3</sub>)  $\delta$  1.25–1.75 (m, 12H), 2.50–2.85 (m, 6H), 3.45 (m, 4H), 4.61 (br, 4H), 4.75 (s, 2H), 6.60 (d, *J* = 10 Hz, 2H), 6.85 (d, *J* = 9 Hz, 1H), 6.95 (d, *J* = 10 Hz, 2H), 7.05

(s, 1H), 7.12 (d,  $J = 9.0$  Hz, 1H); MS (FAB) 431 ( $M^+ + H$ ).

**Iodination of 5 (AMS).** The amine **5** (43 mg, 0.1 mmol) in  $CH_3OH$  (5 mL) was added to 20 mL of 0.5 M sodium acetate buffer (pH 3.3). To this were added 16 mg of NaI (0.11 mmol) in 5 mL of buffer and then 25 mg of chloramine T (0.11 mmol). The mixture was stirred for 5 min, at which time the reaction was stopped by the addition of  $Na_2S_2O_5$  (38 mg, 0.2 mmol) in 10 mL of  $H_2O$ . The aqueous mixture was then extracted with  $4 \times 50$  mL of  $CH_2Cl_2$ . The crude product was subjected to preparative TLC on silica gel GF (20 cm  $\times$  20 cm, eluted with 17:4:1  $CHCl_3/CH_3OH/AcOH$ ) to give the diiodo compound **9** ( $R_f = 0.55$ ):  $^1H$  NMR ( $CDCl_3$ )  $\delta$  1.25–1.85 (m, 12H), 2.45–2.55 (m, 2H), 2.75–3.00 (m, 4H), 3.45 (m, 4H), 4.65 (s, 2H), 4.95 (br, 4H), 6.60 (d,  $J = 9.0$  Hz, 1H), 6.90 (d,  $J = 9.0$  Hz, 1H), 7.05 (s, 1H), 7.45 (s, 1H), 7.55 (s, 1H). Compound **8** ( $R_f = 0.29$ ):  $^1H$  NMR ( $CDCl_3$ )  $\delta$  1.25–1.75 (m, 12H), 2.45–2.60 (m, 6H), 3.45 (m, 4H), 4.60 (br, 4H), 4.75 (s, 2H), 6.60 (d,  $J = 10$  Hz, 2H), 6.95 (d,  $J = 10$  Hz, 2H), 7.05 (s, 1H), 7.55 (s, 1H). Compound **7** ( $R_f = 0.33$ ):  $^1H$  NMR ( $CDCl_3$ )  $\delta$  1.25–1.60 (m, 12H), 2.50–2.75 (m, 6H), 3.45 (m, 4H), 4.60 (br, 4H), 4.75 (s, 2H), 6.70 (d,  $J = 10$  Hz, 1H), 6.83 (d,  $J = 9$  Hz, 1H), 6.98 (dd,  $J = 10$  Hz,  $J = 3$  Hz, 1H), 7.01 (s, 1H), 7.12 (d,  $J = 9$  Hz, 1H), 7.50 (d,  $J = 3$  Hz, 1H); MS (FAB) 557 ( $M^+ + H$ ), 579 ( $M^+ + H + Na$ ).

**Synthesis of Azidosalmeterol 6 (AZS) and Iodoazdosalmeterol 10 (IAS).** Compound **5** or **7** (0.04 mmol) was dissolved in 5 mL of 3 N acetic acid and the mixture treated with  $NaNO_2$  (5 mg, 0.08 mL) in 3 mL of  $H_2O$  at 0 °C for 30 min.  $NaN_3$  (5 mg, 0.08 mmol) in 3 mL of  $H_2O$  was then added, and the reaction mixture was left for 30 min at 0 °C. The reaction was halted by neutralization with concentrated  $NH_4OH$  (1.0 mL) and the mixture extracted with  $CH_2Cl_2$  ( $4 \times 10$  mL). The crude product was purified by preparative TLC (20:4:1  $CHCl_3/CH_3OH/AcOH$ ) to give **6** (14 mg, 77%,  $R_f = 0.61$ ) or **10** (14 mg, 82%,  $R_f = 0.78$ ). For **6**: IR 2100  $cm^{-1}$  ( $N_3$ );  $^1H$  NMR ( $CDCl_3$ )  $\delta$  1.25–1.60 (m, 12H), 2.60 (m, 6H), 3.45 (m, 4H), 4.65 (br, 4H), 4.75 (s, 2H), 6.95 (d,  $J = 9$  Hz, 1H), 6.95 (d,  $J = 10$  Hz, 2H), 7.30 (s, 1H), 7.20 (m, 3H); MS (FAB) 457 ( $M^+ + H$ ). For **10**: IR 2100  $cm^{-1}$  ( $N_3$ );  $^1H$  NMR ( $CDCl_3$ )  $\delta$  1.25–1.75 (m, 12H), 2.50–2.75 (m, 6H), 3.43 (m, 4H), 4.55 (br, 4H), 4.80 (s, 2H), 6.80 (d,  $J = 10$  Hz, 1H), 6.80 (d,  $J = 9$  Hz, 1H), 7.02 (s, 1H), 7.10 (d,  $J = 10$  Hz, 1H), 7.15 (dd,  $J = 9.0$  Hz,  $J = 3$  Hz, 1H), 7.85 (d,  $J = 3$  Hz, 1H); MS (FAB) 583 ( $M^+ + H$ ).

**Radioiodination of 5 (AMS).** To 10  $\mu L$  of 0.1 N NaOH were added 4 mCi of  $Na^{125}I$  (2200 Ci/mmol) in 20  $\mu L$  of 0.1 N NaOH and 30  $\mu L$  of 0.1 N HCl, 60  $\mu L$  of sodium acetate buffer (0.5 M, pH 3.3), 20  $\mu L$  of **5** (3 mM in MeOH), and 5  $\mu L$  of chloramine T (5 mM) in sodium acetate buffer. The reaction was halted after 2 min with 10  $\mu L$  of  $Na_2S_2O_5$  (10 mM in  $H_2O$ ) and the mixture neutralized with 10  $\mu L$  of 5%  $NaCO_3$ . The solution was transferred to a thick-walled conical tube and extracted four times with 500  $\mu L$  of chloroform. The combined chloroform extract was evaporated under a nitrogen stream. The residue was dissolved in 20  $\mu L$  of chloroform and purified by TLC on silica gel (eluted with 17:4:1 methanol/chloroform/acetic acetate) with autoradiography to give **7**. The isolated radioactive product comigrated on TLC with the previously characterized nonradioactive compound.

**Synthesis of [ $^{125}I$ ]IAS 10.** Methanol containing the [ $^{125}I$ ]aminoiodosalmeterol **7** was evaporated with a nitrogen stream, and 50  $\mu L$  of 3 N AcOH was quickly added to the reaction vessel. The reaction mixture was cooled on ice for 15 min. Sodium nitrite (5  $\mu L$ , 0.1 M) was added, and the mixture was cooled for an additional 20 min. Sodium azide (5  $\mu L$ , 0.1 M) was added and the mixture left for 30 min at 0 °C. The reaction was stopped by adding 30  $\mu L$  of concentrated ammonium hydroxide and extracting with chloroform ( $4 \times 300$   $\mu L$ ). The combined chloroform extract was washed twice with brine, concentrated under a nitrogen stream, and immediately dissolved in 30  $\mu L$  of methanol. The radioproduct, [ $^{125}I$ ]IAS, exhibited a single spot which comigrated with the previously characterized nonradioactive compound **10** on a TLC plate.

**Membrane Preparation, Adenylyl Cyclase Activation Assays, and Intact Cell Pretreatment with Salmeterol and IAS.** Membranes containing the human  $\beta_2AR$  were prepared from HEK 293 cells stably transfected with double-epitope-tagged receptor (N-terminal hemagglutinin or C-terminal hexahistidine) by homogenization and a sucrose step gradient as previously described (4). Membrane preparations contained approximately 1–3 pmol of human  $\beta_2AR$  per milligram of membranes, as assessed by [ $^{125}I$ ]iodocyanopindolol binding. Assays for measuring the extent of adenylyl cyclase activation and the effect of pretreating cells with 10 nM salmeterol or IAS were also performed as previously described (4).

**Guinea Pig Trachea Dose–Response and Drug Washout Assays.** Albino female guinea pigs (O'Brien Hybrids, Brooklyn, WI) weighing 450–950 g were housed at the School of Veterinary Medicine in accordance with guidelines approved by the American Association for Accredited Laboratory Animal Care. Guinea pigs were sacrificed using sodium pentobarbital (50 mg/kg, intraperitoneally). Tracheas were removed and cleaned of extraneous tissue while immersed in a physiological salt solution (pH 7.4) with the following composition: 119 mM NaCl, 4.7 mM KCl, 1.0 mM  $NaH_2PO_4$ , 0.9 mM  $MgCl_2$ , 2.5 mM  $CaCl_2$ , 25 mM  $NaHCO_2$ , and 11 mM glucose. Physiological salt solutions used throughout the experiments were aerated with a mixture of oxygen (95%) and carbon dioxide (5%). Proximal trachea (PT) segments consisting of three to four cartilage rings were removed from trachea adjacent to the larynx. Distal trachea (DT) segments consisting of three to four rings were removed either from an area adjacent to the PT of the same trachea or from an area approximately 1 cm distant from the end of the PT. Cartilage rings were suspended in water-jacketed (37–38 °C) 10 mL tissue baths containing the physiological salt solution. Mechanical responses were recorded on a Grass polygraph (model 70, Grass Instruments, Quincy, MA) via force-displacement transducers (FT-03). The resting tension was adjusted to 5g and maintained at the same level during equilibration and drug incubation periods. Rings were allowed to equilibrate prior to any drug addition, during which time the solutions in the baths were replaced with fresh solution about every 10 min.

PT and DT segments from two guinea pigs were used simultaneously in four tissue baths in each of the experiments. Following equilibration of all of the segments connected to the polygraph, the maximum contraction of the tissues was obtained by addition of carbachol to a final concentration of 0.1–1  $\mu M$ . Final maximum responses for



all drugs were taken to be the effects occurring when additional increases in drug concentration failed to elicit a further response. The time required to obtain complete dose-response effects varied with the drug and tissue segment that were used. Cumulative dose-response relaxing effects of salmeterol (on the PT segments) and IAS (on the DT segments) were obtained by increasing concentrations of the added drugs while the previous doses remained in contact with the tissues. Tracheal rings were assumed to be in a maximally relaxed state when further drug addition did not generate more relaxation and after treatment of the tissues with 10  $\mu$ M papaverin.

In a second series of experiments, dose-response experiments were repeated with a slight modification of the procedure described above. Tissues from these experiments were subsequently used for salmeterol and IAS washout studies following equilibration at their respective maximally relaxed state. Starting at time zero and at 5 min intervals until 30 min, while the tissues were still connected to the polygraph, the 10 mL physiological salt solutions contained in each of the tissue baths were replaced with 10 mL of fresh solution containing 1  $\mu$ M carbachol. Differential contractions were measured at the end of each 5 min interval, and the results were calculated as the percentage change relative to the steady state.

**Photoaffinity Labeling of Human  $\beta_2$ AR in HEK 293 Cell Membranes.** Photolabeling of the human  $\beta_2$ AR in membranes from stably transfected HEK 293 cells was performed by incubating membranes at 30 °C for 30 min in the dark with radioligand in the presence or absence of 10  $\mu$ M (–)-alprenolol protector. The membranes were at a protein concentration of approximately 3 mg/mL and were suspended in 100  $\mu$ L of buffer containing 20 mM HEPES and 1 mM EDTA. [<sup>125</sup>I]IAS was added to a final concentration which was between 0.7 and 1.0 nM. Following incubation, membranes were diluted in 5 mL of ice-cold degassed buffer [10 mM Tris, 100 mM NaCl, and 2 mM EDTA (pH 7.4)]. Immediately following dilution, the membranes were photolyzed at 4 °C through a 2 mm thick Pyrex tube for 5 s at a distance of 10 cm from a 1 kW mercury lamp. The membranes were then pelleted by ultracentrifugation at 100000g in a Beckman type 70.1 Ti rotor. The membranes were solubilized in a buffer containing 10 mM Tris (pH 6.8), 2% sodium dodecyl sulfate, 10% glycerol, 5% 2-mercaptoethanol, and 0.05% bromphenol blue dye and subjected to SDS-PAGE on a 12.5% gel. Results were usually obtained with a 48 h autoradiogram using a Quanta III intensifier screen. The molecular mass of the receptor was estimated using the following molecular mass standards: bovine erythrocyte carbonic anhydrase (29 kDa), egg albumin (45 kDa), bovine plasma albumin (66 kDa), rabbit muscle phosphorylase b (97 kDa), *Escherichia coli*  $\beta$ -galactosidase (116 kDa), and rabbit muscle myosin (205 kDa).

**Purification and Proteolysis of [<sup>125</sup>I]IAS-Labeled Human  $\beta_2$ AR.** Following photolysis, the membranes were completely extracted with 400  $\mu$ L of solubilization buffer [1% dodecyl  $\beta$ -D-maltoside, 500 mM NaCl, 20 mM Tris (pH 8.0), 6 M urea, and 5 mM imidazole]. The extract was loaded onto a column of 0.5 mL of nickel affinity resin. The resin was then washed with 10 mL of buffer containing 0.1% dodecyl  $\beta$ -D-maltoside, 10 mM imidazole, 500 mM NaCl, 20 mM Tris (pH 8.0), and 6 M urea, and then again with 5 mL of

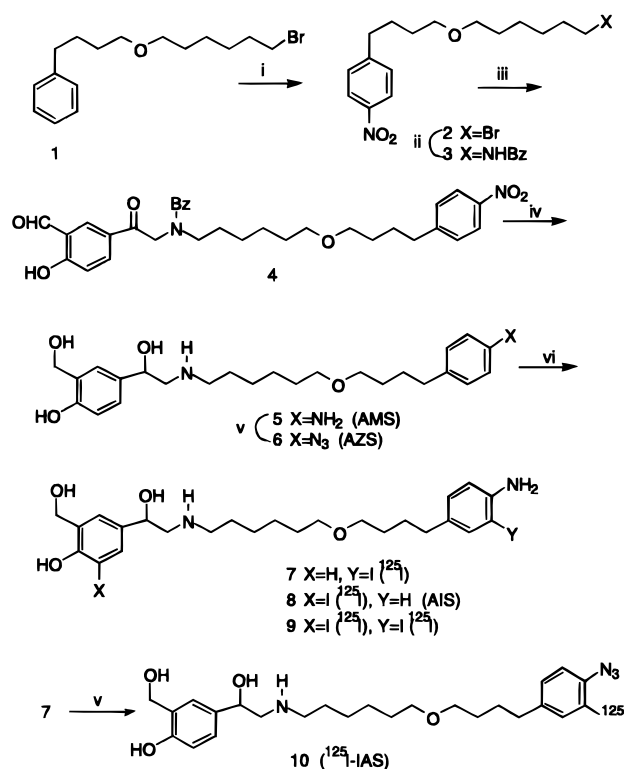


FIGURE 1: Synthesis of salmeterol derivatives and [<sup>125</sup>I]IAS. Reaction conditions were as follows: (i)  $\text{BF}_3\text{NO}_2$ , MeCN; (ii) 5-(bromoacetyl)-2-hydrobenzaldehyde; (iv) (a)  $\text{NaBH}_4$ , MeOH, (b)  $\text{H}_2/\text{Pd-C}$ ; (v)  $\text{NaNO}_2/\text{NaN}_3$ ; (v),  $\text{Na}^{125}\text{I}$ , chloramine T.

Table 1: Effect of Buffer pH on the Product Isomer Distribution<sup>a</sup>

buffer pH	ratio of products <sup>b</sup> 7, 8, and 9	overall % yield
8.6 (1.0 M $\text{K}_2\text{HPO}_4$ )	0:1.0:1.7	56
7.3 (1.0 M $\text{K}_2\text{HPO}_4$ )	0:1.0:1.3	43
5.6 (0.5 M $\text{NaOAc}$ )	1.0:2.2:1.8	50
3.3 (0.5 M $\text{NaOAc}$ )	1.5:1.0:1.2	58
2.1 (1.0 M $\text{HOAc}$ )	1.3:1.0:1.0	47

<sup>a</sup>  $\text{NaI}$ /chloramine T/aminosalmeterol ratio of 1:1:1. <sup>b</sup> For products, see Figure 1.

buffer containing 0.1% dodecyl  $\beta$ -D-maltoside, 10 mM imidazole, 500 mM NaCl, and 20 mM Tris. The  $\beta_2$ AR was eluted using 4 mL of buffer containing 0.1% dodecyl  $\beta$ -D-maltoside, 250 mM imidazole, 500 mM NaCl, and 20 mM Tris (pH 8.0). The eluate was concentrated using a Centricon concentrator, and the residue was eluted in 100  $\mu$ L of a buffer containing 20 mM Tris (pH 7.4) and 250 mM NaCl. Factor Xa protease was added to the purified photolabeled receptor solutions to a final concentration of 10  $\mu$ g/mL and incubated at 30 °C for 12 h. Proteolysis was terminated by adding sample buffer containing 10 mM Tris (pH 6.8), 2% sodium dodecyl sulfate, 10% glycerol, 5% 2-mercaptoethanol, and 0.05% bromphenol blue dye and the solution electrophoresed via 12% SDS-PAGE, followed by autoradiography.

## RESULTS

**Synthesis of the Photoaffinity Label [<sup>125</sup>I]IAS.** The synthetic scheme and structure of [<sup>125</sup>I]IAS are shown in Figure 1. The product was prepared first in a nonradioactive form and then in a carrier-free form with <sup>125</sup>I. The nonradioactive compounds were used for chemical characterization and

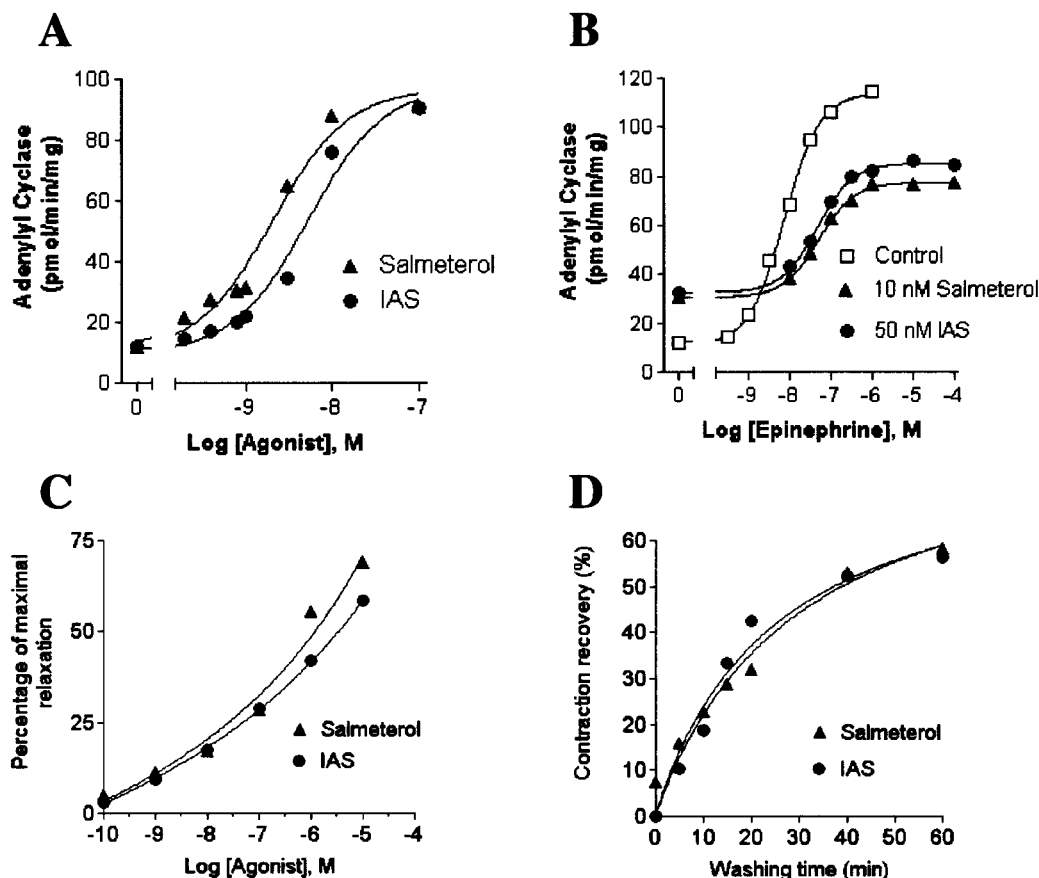


FIGURE 2: Comparison of salmeterol and IAS activity in multiple assay systems. (A) Comparison of  $\beta_2$ AR-mediated salmeterol and IAS stimulation of adenylyl cyclase in HEK 293 membrane preparations. The dose-response experiment of adenylyl cyclase stimulation for salmeterol and IAS was performed as described in Materials and Methods. Assays were performed in triplicate, and the standard error of the mean of triplicates did not exceed 10%. Incubations with agonists were carried out 10 min at 30 °C. (B) Effect of pretreatment of HEK 293 cells with salmeterol or IAS on epinephrine activation of adenylyl cyclase. HEK 293 cells were pretreated for 5 min with carrier (controls), 10 nM salmeterol, or 10 nM IAS in complete growth medium at 37 °C, washed six times with phosphate-buffered saline, and homogenized, after which membranes were isolated on sucrose step gradients. Adenylyl cyclase assays were performed with various concentrations of epinephrine as indicated. The  $EC_{50}$ s for epinephrine activation were 7.1, 48, and 44 nM for control, salmeterol-pretreated, and IAS-pretreated conditions, respectively. Assays were performed in triplicate, and the given values are the means from one experiment. (C) Dose-response curves for the relaxation of carbachol-contracted guinea pig tracheal segments with salmeterol and IAS. Data that are shown are the average from eight separate experiments and are expressed as a percentage of relaxation relative to full relaxation by 10  $\mu$ M papaverin. (D) Comparison of the relaxation recovery of carbachol-contracted guinea pig trachea with salmeterol and IAS as a function of washing time ("drug washout experiment"). Salmeterol ( $10^{-5}$  M) and IAS ( $10^{-5}$  M) were shown to be equally resistant to drug washout, and by this measure to have equivalent exosite binding properties.

adenylyl cyclase assays, whereas the radioiodinated compound was used for photolabeling. The synthetic protocol for AMS (compound **5**) was similar to that for salmeterol described previously (10), except for preparation of nitro compound **2** (11). Treatment of compound **1** proceeded smoothly with nitronium tetrafluoroborate to give *p*-nitro compound **2** and the *o*-nitro isomer. Para product **2** was separated from its *o*-nitro isomer by silica gel column chromatography.

The iodination of AMS **5** proved to be complicated. From the structure of compound **5**, illustrated in Figure 1, there are two phenyl rings which are both activated by either hydroxyl groups or an amino group and can be accessed by iodine. Three iodinated products were isolated and identified as the two monoiodinated compounds **7** and **8** and the diiodinated product **9** from their spectral properties. We found that the isotopomer distribution was directly controlled by the reaction buffer pH (Table 1). The difficulty in generating the desired compound **7** in which the iodine is located on the aminophenyl ring as a major product is the

fact that the saliginin ring is much more reactive to iodination than the aminophenyl ring. As shown in Table 1, a range of pH values from 8.6 to 2.1 were tested, and an acidic condition was found which slightly favors formation of **7**. The radioiodinated amine **7** was isolated and purified by TLC. The purified compound **7** was shown to comigrate on TLC with the identical nonradioactive compound. Conversion of the aminobenzyl group in the salmeterol derivatives to the corresponding azide compound **10** ( $[^{125}\text{I}]\text{IAS}$ ) proceeded readily via the diazonium salt intermediate prepared in 3 N acetic acid. Carrier-free  $[^{125}\text{I}]\text{IAS}$  was stable in methanol at -20 °C for at least 3 weeks.

**Cell-Free Activation of Adenylyl Cyclase in HEK 293 Cell Membranes by Salmeterol, IAS, and Related Derivatives.** The characteristics of salmeterol activation of adenylyl cyclase have previously been reported (3, 4). IAS was tested to determine whether it would exhibit the same activation properties as the parent drug, salmeterol. Figure 2A shows that the dose-response curves for  $\beta_2$ AR-mediated cyclase activation by salmeterol and IAS were similar, displaying

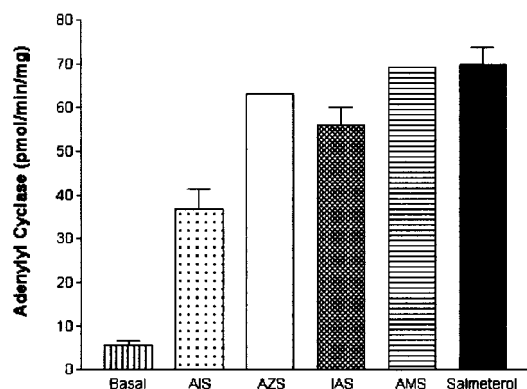


FIGURE 3: Activation of adenylyl cyclase by salmeterol and various analogues (compounds **5**, **6**, **8**, and **10** shown in Figure 1). Adenylyl cyclase assays were performed as described in Materials and Methods. Assays were performed in triplicate, and the values that are shown are the mean  $\pm$  the range of two separate assays. All of the compounds were assayed at a concentration of 10 nM.

EC<sub>50</sub>s of 2 and 5 nM, respectively. Figure 3 demonstrates that, in addition to IAS, salmeterol-like agonist activity could also be demonstrated with AMS (compound **5**) and AZS (compound **6**). In the experiment whose results are depicted in Figure 3, all agonists were at a concentration of 10 nM and no additional activation was observed with 100 nM drug. The iodinated isomer AIS **8** which contained the iodine on the saligenin ring had approximately 50% of the activity of salmeterol. The reduced activity of the iodinated saligenin derivative **8** (AIS) is not surprising since the bulky iodine atom is likely to interfere with interaction of the saligenin head with the  $\beta_2$ AR catechol binding site.

**Comparison of the Effect of Pretreatment of HEK 293 Cells with Salmeterol or IAS on the Subsequent Activation of Adenylyl Cyclase with the Full Agonist Epinephrine.** In an assay in which the effect of agonist pretreatment on the subsequent ability of epinephrine to stimulate the  $\beta_2$ AR was being measured, both salmeterol and IAS behaved essentially the same (Figure 2B). The activity with no added epinephrine represents the amount of drug carried over from the pretreatment which is not readily removed by the washes and membrane purification procedure, and was identical for both salmeterol and IAS. The increased EC<sub>50</sub> and decreased V<sub>max</sub> for epinephrine stimulation are caused by a combination of drug-induced desensitization from the pretreatment and competition of salmeterol or IAS for the active site due to residual drug from exosite binding and/or partitioning into the lipid. The properties of both salmeterol and IAS in this assay are the same as those previously reported for salmeterol (4).

**Guinea Pig Trachea Relaxation Dose-Response and Washout Assay.** Tissue segments from adult guinea pig tracheas were used to compare dose responses when the guinea pigs were treated with various concentrations of salmeterol and IAS (Figure 2C). Tissues were also used to compare washout experiments when salmeterol and IAS were used. Pooled data showed no significant differences in the resistance to washout of these two compounds (Figure 2D), indicating that salmeterol and IAS have equivalent exosite binding properties.

**Photoaffinity Labeling of the  $\beta_2$ AR in HEK 293 Cell Membranes.** A facile synthesis of carrier-free radioiodinated IAS is outlined in Figure 1. When [<sup>125</sup>I]IAS was used in

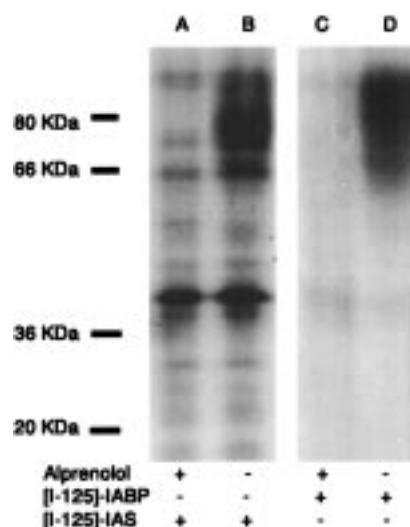


FIGURE 4: Photolabeling of the  $\beta_2$ AR in HEK 293 membranes with [<sup>125</sup>I]IAS and the  $\beta_2$ AR antagonist photolabel, [<sup>125</sup>I]IABP. HEK 293 membranes (2.9  $\mu$ g/ $\mu$ L) were incubated with [<sup>125</sup>I]IAS (1 nM) or [<sup>125</sup>I]IABP (30–60 pM) for 30 min at 30 °C in the presence (A and C) or absence (B and D) of 10<sup>-5</sup> M (–)-alprenolol. The results show both agonist and antagonist photoaffinity labeling of the  $\beta_2$ -AR (the broad band around 70–80 kDa).

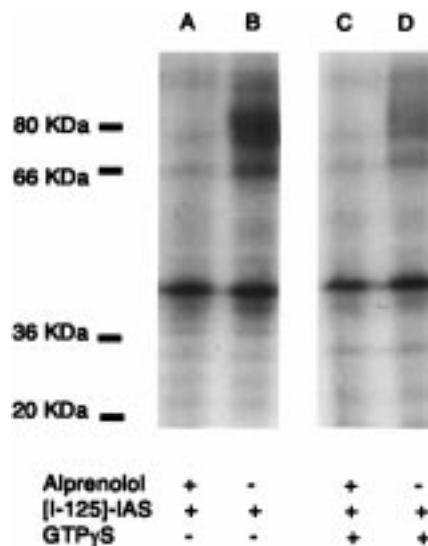


FIGURE 5: Guanylyl nucleotide sensitivity of [<sup>125</sup>I]IAS photolabeling. [<sup>125</sup>I]IAS (1 nM) was incubated in the presence (A and C) or absence (B and D) of (–)-alprenolol (10<sup>-5</sup> M). The incubation time with [<sup>125</sup>I]IAS was 30 min. The addition of GTP $\gamma$ S (10<sup>-4</sup> M) (C and D) resulted in significant reduction of the extent of specific labeling.

photoaffinity labeling experiments using partially purified HEK 293 cell membranes (Figure 4), alprenolol-protectable photolabeling of the  $\beta_2$ AR could readily be demonstrated (broad glycosylated band seen at approximately 70–80 kDa; see lanes A and B of Figure 4). To further confirm that the broad band at 70–80 kDa was indeed the  $\beta_2$ AR, photolabeling of a separate aliquot of the same membranes was also performed using the high-affinity  $\beta_2$  antagonist photolabel, [<sup>125</sup>I]IABP (12) (see lanes C and D of Figure 4). The extent of labeling of the  $\beta_2$ AR with [<sup>125</sup>I]IAS is greatly reduced by the presence of GTP $\gamma$ S (see Figure 5; compare lanes C and D relative to control lanes A and B). The reduction of the extent of [<sup>125</sup>I]IAS photolabeling by addition of GTP $\gamma$ S suggests a decrease in agonist affinity caused by



dissociation of the G-protein–receptor complex. This corresponded with previous results which showed that salmeterol displays a GTP shift, consistent with it being a very weak partial agonist. These data indicate that IAS interacts with the receptor as an agonist and that exosite photolabeling in the receptor binding site occurred primarily as the ternary IAS–receptor–G-protein complex.

**Purification and Proteolysis of the  $\beta_2$ AR.** IAS-labeled  $\beta_2$ AR from HEK 293 membranes was purified by nickel affinity chromatography as described in Materials and Methods. The  $\beta_2$ AR was specifically photolabeled in an alprenolol-protectable manner by both [ $^{125}$ I]IABP (Figure 6, lanes A and B) and [ $^{125}$ I]IAS (Figure 6, lanes C and D). In the large intracellular loop III of human  $\beta_2$ AR, the amino acid sequence SEGR is cleaved by factor Xa protease (13). A proteolytic cleavage at this site in the  $\beta_2$ AR generates two fragments; one fragment includes the glycosylated N-terminus and first five TM segments, and the other fragment (approximately 21 kDa) contains TM segments 6 and 7 and the C-terminus (Figure 6). Factor Xa digestion of the control [ $^{125}$ I]IABP-labeled receptor generated two radiolabeled peptides: a highly glycosylated peptide containing helices 1–5 (broad, glycosylated band around 50–60 kDa; Figure 6, lanes E and F) and a smaller peptide containing TMs 6 and 7 (sharp band around 21 kDa; Figure 6, lanes E and F) consistent with previous results (1, 14). In contrast, however, factor Xa cleavage of the [ $^{125}$ I]IAS-derivatized receptor revealed essentially all of the label only on the smaller C-terminal peptide containing TMs 6 and 7 (Figure 6, lanes G and H). This was further confirmed by showing that this small C-terminal polyhistidine-tagged peptide bound to a nickel affinity column following proteolysis and could be eluted with 300 mM imidazole (Figure 6, lanes I–N). Considering that the photoactive azide moiety is positioned on the ring at the end of the long hydrophobic portion of salmeterol which confers long functional activity, and which is hypothesized to be involved in exosite binding, we conclude that if there is a high-affinity exosite on the receptor, and at least a portion of this may be contributed by the fragment which contains TM segments 6 and 7.

## DISCUSSION

Salmeterol and certain other long-chain antagonists and agonists of the  $\beta_2$ AR have unusual properties. These properties involve a prolonged agonist action on the receptor even after removal of excess salmeterol, which can be inhibited by antagonists but recovers its agonist properties following removal of antagonist (2, 15, 16). Salmeterol possesses a very high coefficient for partitioning between the hydrophobic and aqueous environments which has led to the hypothesis that the long-acting properties of salmeterol are due to access to the  $\beta_2$ AR binding site from within the bilayer (6, 7), and recent kinetic studies may support this proposal (9). However, support for the presence of a specific exosite found on the  $\beta_2$ AR is suggested by two lines of evidence. First, salmeterol exosite binding is specific to the  $\beta_2$ AR. When recombinant human  $\beta_1$ ,  $\beta_2$ , and  $\beta_3$  receptors were transfected into CHO cells, the only receptor which demonstrated persistent, exosite binding salmeterol kinetics was the  $\beta_2$ AR (16). Second, exosite binding cannot be entirely a function of the lipophilic character of salmeterol. A series of salmeterol-like molecules were synthesized in which the

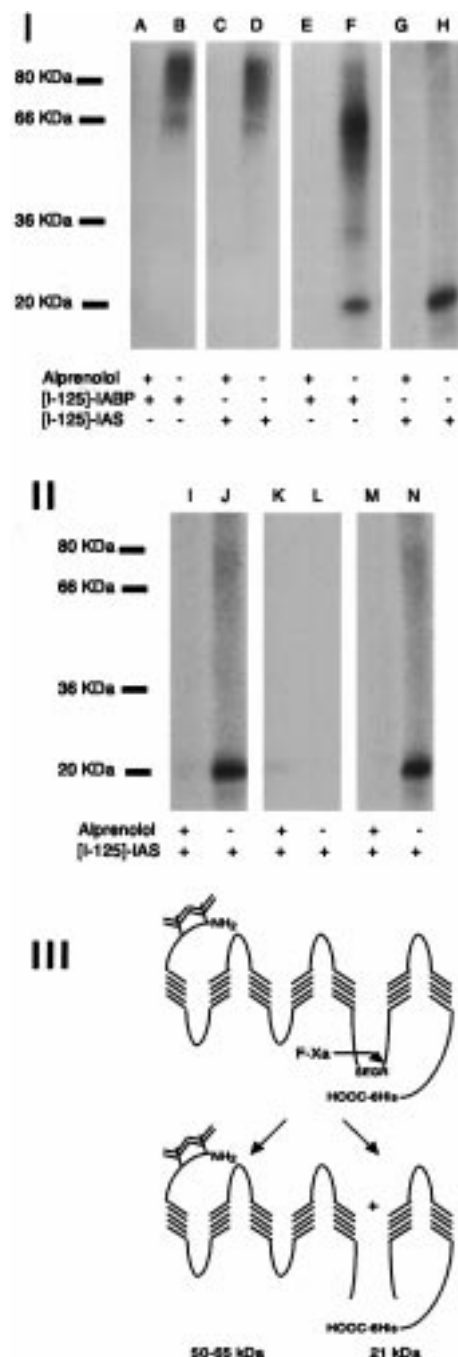


FIGURE 6: (I) Factor Xa cleavage of [ $^{125}$ I]IABP- and [ $^{125}$ I]IAS-labeled human  $\beta_2$ AR. Polyhistidine-tagged  $\beta_2$ AR expressed in HEK 293 cell membranes was photolabeled with [ $^{125}$ I]IABP and [ $^{125}$ I]IAS and purified using nickel affinity resin (lanes A–D). The labeled  $\beta_2$ AR was then treated with factor Xa protease. Lanes E and F contained the two radioactive peptides from [ $^{125}$ I]IABP-labeled  $\beta_2$ AR. In lanes G and H, only the smaller C-terminal peptide was labeled by [ $^{125}$ I]IAS. (II) The C-terminal, IAS-photolabeled peptide can bind to and be eluted from a nickel column. Shown is factor Xa-cleaved  $\beta_2$ AR that had been previously photolabeled in the presence (lane I) or absence (lane J) of alprenolol protector. These were loaded onto nickel resin and washed with 20 column volumes of low-imidazole buffer. No labeled peptide eluted in the washes (lanes K and L). The columns were then eluted with 300 mM imidazole (lanes M and N), and the alprenolol protectably labeled peptide was recovered. (III) Diagram of the  $\beta_2$ AR showing the location of the factor Xa cleavage site, and the size of the two fragments generated after cleavage.

position of the ether oxygen was moved along the long-chain saturated hydrocarbon tail. Within the saturated hydrocarbon

tail, salmeterol has six methylene groups on one side of the ether oxygen and four methylenes on the other ("6 and 4"). The salmeterol-like molecules had the same number of methylenes, but the position of the ether oxygen was different ("4 and 6", "5 and 5", "2 and 8", "8 and 2", or "9 and 1"). All of these molecules had the very same partition coefficient, but their reported duration of action varied widely. Salmeterol ("6 and 4") had the longest duration of action (>720 min), while the shortest acting molecule was the "2 and 8" compound (2.7 min) (2). Specificity in both the receptor and the position of the ether oxygen suggests distinct exosite binding determinants, i.e., an exosite which is contained at least in part within the specific sequences of the  $\beta_2$ AR.

On the basis of the initial observation that, unlike the  $\beta_2$ -AR, the  $\beta_1$ AR does not exhibit salmeterol exosite binding behavior, Green et al. (5) addressed the question of the molecular basis of the salmeterol exosite by substituting portions of the  $\beta_1$  receptor into the  $\beta_2$  receptor and testing for exosite binding activity in drug washout experiments. They identified a sequence of amino acids in TM 4 that had some effect on exosite binding. When the  $\beta_1$  sequence was placed into the  $\beta_2$  receptor, the extent of exosite binding was diminished by approximately two-thirds. In the reverse chimera, when the  $\beta_2$  sequence was placed into the  $\beta_1$  receptor, a degree of exosite binding activity was recovered. While those authors did not specifically suggest that any other particular sites on the  $\beta_2$ AR contribute to exosite binding, they recognized the fact that there may be other sites on the receptor which contribute to exosite interactions.

We chose to take a biochemical approach to locating the salmeterol binding site. Since the exosite binding behavior of salmeterol is attributed to the long *N*-aryloxyalkyl side chain, it was logical to identify the position of the phenyl ring at the end of this long chain by placing a photomoiety at this location in the molecule. A novel salmeterol-based photolabel ([<sup>125</sup>I]IAS) with the photoactivatable azide group positioned on the exosite binding portion of the molecule was synthesized and used to label the  $\beta_2$ AR, and the labeled receptor was cleaved at a unique known site into a large N-terminal and a small C-terminal peptide. All of the IAS label was only on the portion of the  $\beta_2$ AR which contains TMs 6 and 7, and not on the larger fragment, which includes TM 4. As in the case of the sequence identified by Green et al. in the cytoplasmic half of TM 4, there are also a number of amino acid differences between the  $\beta_1$ AR and the  $\beta_2$ AR in the extracellular halves of TM 6 and TM 7, and these may also contribute to the differences in the exosite binding activity between these two receptors. Recently, it has been demonstrated by construction of chimeric receptors and site-directed mutagenesis that residues in TM 7 do in fact contribute to salmeterol high-affinity binding. Kurose et al. (17) took advantage of the great difference in salmeterol binding affinities between the  $\beta_1$ -adrenergic receptor (2200 nM) and the  $\beta_2$ -adrenergic receptor (1.5 nM) by constructing chimeric receptors and testing salmeterol binding affinity to determine which portions of the receptor were responsible for the difference in binding affinity. After TM 7 of the  $\beta_2$ -adrenergic receptor was replaced with the corresponding segment from the  $\beta_1$ -adrenergic receptor, the affinity for salmeterol changed completely from being  $\beta_2$ -like (high-affinity) to being  $\beta_1$ -like (low-affinity). When the reverse chimera was constructed (TM 7 of the  $\beta_2$ -adrenergic receptor

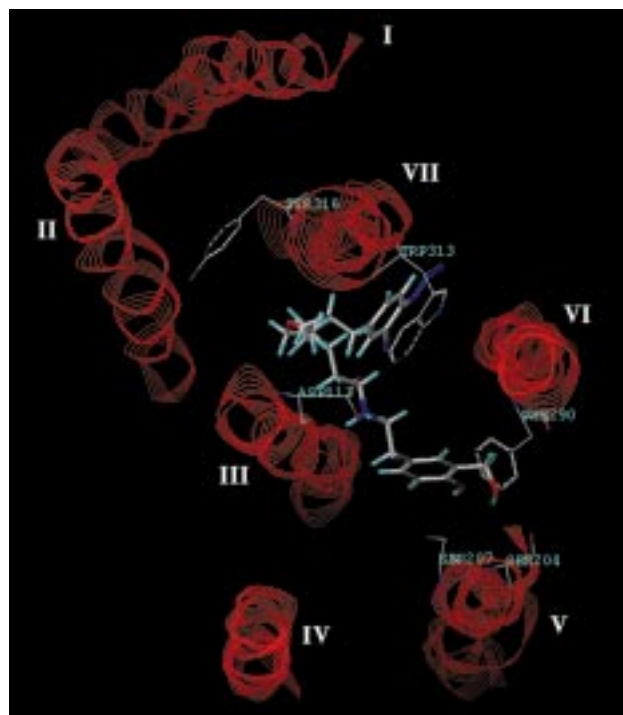


FIGURE 7: Speculative model of the binding of IAS to the  $\beta_2$ AR. The  $\beta_2$ AR TM helices are from the model of Donnelly et al. (18) obtained from the EMBL G-protein-coupled receptor database (19). Elements incorporated in this model include the catechol hydroxyls within hydrogen bonding distance of serines 205 and 207 in TM 5, the amine interaction with aspartic acid 113 in TM 3, and the photoaffinity labeling data from this paper, which demonstrate that the iodoazidophenyl ring of IAS is near TM 6 or TM 7.

placed into a  $\beta_1$ -adrenergic receptor background), a large measure of the high-affinity binding was regained. This molecular biological evidence for important salmeterol binding determinants existing in TM 7 is consistent with the biochemical data for iodoazidosalmeterol photolabeling presented in this report. Kurose et al. further introduced mutations of 10 amino acids in TM 7 that were different between these two adrenergic receptor subtypes, and found that mutation of the single amino acid tyrosine 308 (in the  $\beta_2$ -adrenergic receptor) to alanine led to an approximate 100-fold decrease in salmeterol affinity, but not the entire 1500-fold change seen in the chimera when the entire transmembrane segment was replaced. This suggests that multiple residues in TM 7 contribute to salmeterol binding affinity and is consistent with the IAS photoaffinity labeling results. The possibility exists that multiple regions of the receptor and also some component of lipid bilayer interaction may contribute to exosite binding interactions with salmeterol and, more specifically, that the interaction of the salmeterol hydrophobic tail with TM 6 and/or TM 7 may contribute incrementally to the binding affinity, and hence serve minimally as an exosite. With the IAS photolabel as a tool, we are now in a position to assess directly whether IAS remains "tethered" at the  $\beta_2$ AR in the presence of a function-blocking concentration of antagonist, and these experiments are now underway.

It is widely accepted that serines 204 and 207 in TM 5 and aspartic acid 113 in TM 3 interact with the hydroxyl groups and the amine, respectively, of  $\beta_2$ AR ligands, including salmeterol. Recently, it has been proposed that the ether oxygen of the *N*-aryloxyalkyl side chain of salmeterol



may interact with tyrosine 316 in TM 7 (17). The photoaffinity labeling data presented in this paper demonstrate that the iodoazidophenyl ring of IAS photoincorporates into either TM 6, TM 7, or both. When this information is taken together, a model of the manner in which salmeterol may bind to the  $\beta_2$ AR can be hypothesized (Figure 7). The Donnelly model for the human  $\beta_2$ AR TM segments (18) was obtained from the EMBL G-protein-coupled receptor database (19). Modeling was carried out on a Silicon Graphics O<sub>2</sub> computer using the program Sybyl (Tripos, St. Louis, MO). We have modeled the iodoazidophenyl ring of IAS as interacting with Trp 313, which was found to be the photoincorporation site for the antagonist photoaffinity label, IABP, in the turkey erythrocyte  $\beta$  receptor (14). If IAS does interact at the same site on TM 7 as the shorter photolabel IABP, it would suggest a partially folded conformation for salmeterol, which does not seem unreasonable to us; however, this is speculation. An equally reasonable hypothesis may be that salmeterol interaction occurs on the opposite face of TM 7 with Tyr 308. Support for this alternative hypothesis comes from the fact that when mutated to Ala, Tyr 308 was found to be responsible for approximately 10% of the difference in binding affinity between the  $\beta_2$ AR (high affinity) and the  $\beta_1$ AR (low affinity) (17). Modeling is limited because there is no high-resolution structure of the receptor available and because the precise amino acid where IAS reacts has not yet been determined. However, at present we hypothesize that photolabeling occurs in the extracellular half of TM 6 or 7, rather than in the intracellular half. One reason for this prediction is that the  $\beta_1$ AR, which does not exhibit long-acting salmeterol exosite binding behavior, differs significantly from the  $\beta_2$ AR in the extracellular halves of both TM 6 and TM 7, but less so in the intracellular halves of these TM segments, possibly suggesting that unique salmeterol binding determinants are in the extracellular half of TM 6 and/or TM 7.

IAS was thoroughly compared to salmeterol in both a cell-free adenylyl cyclase assay and a tissue-based assay. IAS exhibited properties nearly identical to those of salmeterol for activation of adenylyl cyclase (2–3-fold increased EC<sub>50</sub>) in a cell-free assay, and exhibited similar effects of pretreatment on subsequent assays of epinephrine stimulation. IAS also exhibited the same dose–response curve and drug washout kinetics as salmeterol in perfused guinea pig trachea assays.

The salmeterol derivatives that are reported in this paper (Figure 1) represent a unique approach to the synthesis of this compound and its analogues. This approach was based on a synthesis of salmeterol which we have recently described (10). The primary feature of the synthetic scheme is the relative simplicity of the approach, which has allowed us to prepare multiple derivatives of salmeterol, namely, amino substituted, azido substituted, and iodoazido substituted in a relatively straightforward fashion.

In summary, we have developed a novel photoaffinity probe [<sup>125</sup>I]IAS, in which the photoactivatable azide is at the extreme end of the salmeterol *N*-aryloxyalkyl chain which confers the very long-acting properties to this compound. A specific region of the  $\beta_2$ AR containing TM 6 and 7 is labeled by this compound in an alprenolol-protectable manner. These results expand the current view of the salmeterol binding site and suggest a method for the future work of directly testing the exosite hypothesis using this novel photolabel. These results may provide useful information concerning the manner in which other G-protein-coupled receptor ligands could be rendered long-acting agonists or antagonists.

## ACKNOWLEDGMENT

We thank Dr. Ricardo Saban (University of Wisconsin School of Veterinary Medicine) for assistance with the guinea pig tracheal tissue assays and Jackie Friedman (University of Texas Health Science Center at Houston) for performing the adenylyl cyclase assays.

## REFERENCES

- Hockerman, G. H., Girvin, M. K., Malbon, C. C., and Ruoho, A. E. (1996) *Mol. Pharmacol.* 49, 1021–1032.
- Johnson, M. (1995) *Med. Res. Rev.* 15, 225–257.
- Clark, R. B., Allal, C., Friedman, J., Johnson, M., and Barber, R. (1996) *Mol. Pharmacol.* 49, 182–189.
- January, B., Seibold, A., Allal, C., Whaley, B. S., Knoll, B. J., Moore, R. H., Dickey, B. F., Barber, R., and Clark, R. B. (1998) *Br. J. Pharmacol.* 123, 701–711.
- Green, S. A., Spasoff, A. P., Coleman, R. A., Johnson, M., and Liggett, S. B. (1996) *J. Biol. Chem.* 271, 24029–24035.
- Anderson, G. P., Linden, A., and Rabo, K. F. (1994) *Eur. Respir. J.* 7, 569–578.
- Rhodes, D. G., Newton, R., Butler, R., and Herbet, L. (1992) *Mol. Pharmacol.* 42, 596–602.
- Lofdahl, C. (1990) *Lung* (Suppl.), 18–22.
- Teschemacher, A., and Lemoine, H. (1999) *J. Pharmacol. Exp. Ther.* 288, 1084–1092.
- Rong, Y., and Ruoho, A. E. (1999) *Synth. Commun.* 29, 2155.
- Carroll, F. I., Gao, Y., Rahman, M., Abraham, P., Parham, K., Lewin, A., and Boja, J. (1991) *J. Med. Chem.* 34, 2719–2725.
- Rashidbaigi, A., and Ruoho, A. E. (1981) *Proc. Natl. Acad. Sci. U.S.A.* 78, 1609–1613.
- Wu, Z., and Ruoho, A. E., unpublished results.
- Wong, L. K. F., Slaughter, C., Ruoho, A. E., and Ross, E. M. (1988) *J. Biol. Chem.* 263, 7925–7928.
- Nials, A. T., Summer, M. J., Johnson, M., and Coleman, R. A. (1993) *Br. J. Pharmacol.* 108, 507–515.
- Ball, D. I., Brittain, R. T., Coleman, R. A., Denyer, L. H., Jack, D., Johnson, M., Lunts, L. H. C., Nials, A. T., Sheldrick, K. E., and Skidmore, I. F. (1991) *Br. J. Pharmacol.* 104, 665–671.
- Isogaya, M., Yamagiwa, Y., Fujita, S., Sugimoto, Y., Nagao, T., and Kurose, H. (1998) *Mol. Pharmacol.* 54, 616–622.
- Donnelly, D., Findlay, J. B. C., and Blundell, T. L. (1994) *Recept. Channels* 2, 61–78.
- Horn, F., Weare, J., Beukers, M. W., Hörsch, S., Bairoch, A., Chen, W., Edvardsen, Ø., Campagne, F., and Vriend, G. (1998) *Nucleic Acids Res.* 26, 277–281.

BI9910676